^{210}Pb in the ocean: A pilot tracer for modeling particle reactive elements

ERNST MAIER-REIMER[1] and GIDEON HENDERSON[2]

[1] *Max-Planck-Institut für Meteorologie, Bundesstr. 55, 20146 Hamburg, Germany*
[2] *Lamont-Doherty Earth Observatory, Palisades, N.Y, 10964, USA*
e-mail: maier-reimer@dkrz.de

We discuss the basic requirements for a successful modeling of ^{210}Pb in the ocean as a test tracer for at least other lead isotopes, but also of other elements that behave similarly to lead. With the aid of realistic models of the oceanic circulation and the major biogeochemical cycles in it, the result is a dynamically consistent model of lead cycling that reproduces observed profiles within 10%.

1. Introduction

Stable Pb-isotope ratios such as ^{207}Pb/^{204}Pb show spatial variability in the oceans. This is expected from the fact that the Pb-isotope composition of continental crust varies around the globe and as lead has a residence time in the oceans significantly shorter than the mixing time. The natural variation in Pb isotopes in the oceans has been observed by observations in manganese nodules and crusts (Abouchami and Goldstein 1995; von Blanckenburg 1996). And variation in Pb isotope ratios through geological time at a single site is also known to occur from studies of manganese crusts (Christensen *et al* 1997; O'Nions *et al* 1998). The Pb isotope ratio pattern in the ocean is controlled by the distribution of inputs of Pb to the ocean, the advection of Pb by ocean circulation, and the removal of Pb by scavenging onto sedimenting particles. The Pb isotope distribution in the past ocean therefore has the potential to provide information about the distribution of continental weathering in the past, ocean circulation in the past, and ocean-productivity in the past. But deconvolving these three effects from the Pb-isotope record is problematic. This problem is compounded by the fact that, in the modern ocean, Pb-isotopes are almost entirely controlled by anthropogenic aerosol contamination. This prevents us from using the modern as the key to the past in our attempts to understand the controls on Pb-isotopes in the oceans. Lead also has a short lived isotope, ^{210}Pb, which is not significantly anthropogenically perturbed. In this study, we modelled the input, advection, and removal of ^{210}Pb in an ocean GCM in order to better understand the controls on the natural Pb distribution in the ocean. This study also represents an early attempt to introduce particle-reactive elements to an ocean GCM and may therefore be more widely applicable to the many elements which exhibit this behaviour in seawater.

^{210}Pb (half-life 22.3 years) is a decay product of the ^{238}U -series with intermediate products ^{234}Th, ^{234}Pa, ^{234}U, ^{230}Th (half-life 75,000 years) and ^{226}Ra (half-life 1600 years). The subsequent transitions (^{222}Rn, ^{218}Po, ^{214}Pb, ^{214}Bi, ^{214}Po) to ^{210}Pb are so fast that the decay of ^{226}Ra can be taken locally as source for ^{210}Pb. Another source is from eolian transport of ^{222}Rn (half-life 3.8 days) that emanates from continental crusts. The strength of this source is rather well established by the use of well calibrated atmospheric transport models (Preiss and Genthon 1997). In the ocean, lead tends to attach to biogenic particles and to become buried in sediments (Cochran *et al* 1990). Modeling ^{210}Pb as an isolated study would be a rather hopeless task: ocean circulation, particle fluxes and the distribution of ^{226}Ra, of which only sparse data are available, must be specified as input data. Ultimately, these input fields must be provided by precursor models that are validated individually. The present

Keywords. Lead isotopes; ^{210}Pb; tracer; reactive elements; oceanic circulation.

Proc. Indian Acad. Sci. (Earth Planet. Sci.), **107**, No. 4, December 1998, pp. 351–357

study is based on the Hamburg model of the oceanic carbon cycle (HAMOCC3, Maier-Reimer 1993) which itself is based on a model of physical circulation (LSG, Maier-Reimer *et al* 1993).

From the applications of the model to date, we see a classification of tracers into four categories, listed in order of increasing importance of the role of circulation models for the interpretation of data:

I) Dense data of the dynamically active tracers T, S, which determine velocity. A model like ours is of little value for an "explaining" description of the data; it is useful primarily for an estimate of the sensitivity of the circulation with respect to changing surface conditions. These hydrographic fields are, of course, the base of all modeling efforts. It is, however, an old dilemma dating from the time when the first diagnostic models were constructed by Sarkisyan (1969), that the available data (Levitus 1983) – collected over many decades – are not fully compatible with a plausible circulation pattern. Toggweiler *et al* (1989) pointed out that a purely prognostic run with their circulation model produced moderately realistic distributions of T, S, and radiocarbon, whereas their "robust diagnostic" run with internal restoring to observed hydrography produced a very unrealistic distribution of radiocarbon.

II) Moderately sparse physical tracer data such as PO_4. (see below), ^{14}C from bombs and cosmic rays, CFC's, ^{3}H, ^{3}He from known sources provide a check of circulation. After determining the checks to be successful, the model can be taken for interpolation in space and time and for computation of inventories.

III) Moderately sparse biogenic tracer data for PO_4, alkalinity, ΣCO_2, $Si(OH)_4$, O_2 react on the circulation and weakly on biological parametrization. Once the physical circulation of the model is accepted, the model is applied to determine the strength of the biological pumping mechanism. Successful modeling of $\delta^{13}C$ and the depth of the lysocline is essential for constraining models of past circulation states by the sedimentary records.

IV) Exotic tracers in our definition are, for example ^{39}Ar, ^{3}He from ridge crests, ^{32}Si from cosmic rays, lead isotopes, anthropogenic CO_2, etc. They are characterized either by the sparseness of data or by the lack of knowledge about the sources or by the difficulties of the measurements. In this category models provide essential tools to interpret the data, either by narrowing the uncertainties of source and sink mechanisms, or even by questioning the reliability of data (e.g. Peng *et al* 1993).

2. The source from ^{226}Ra

Since Thorium is very quickly scavenged out from the water, the main source for Radium is deep sea-floor regions with low sediment accumulation rates; at locations with high accumulation rates, Th has partly entered sedimentary diagenesis below the bioturbated layer before releasing its decay product to the water column.

From GEOSECS we have available 845 data points for ^{210}Pb and 591 for ^{226}Ra. Reconstruction and mapping of the three-dimensional structure is, thus, not trivial. Standard procedures of objective mapping are

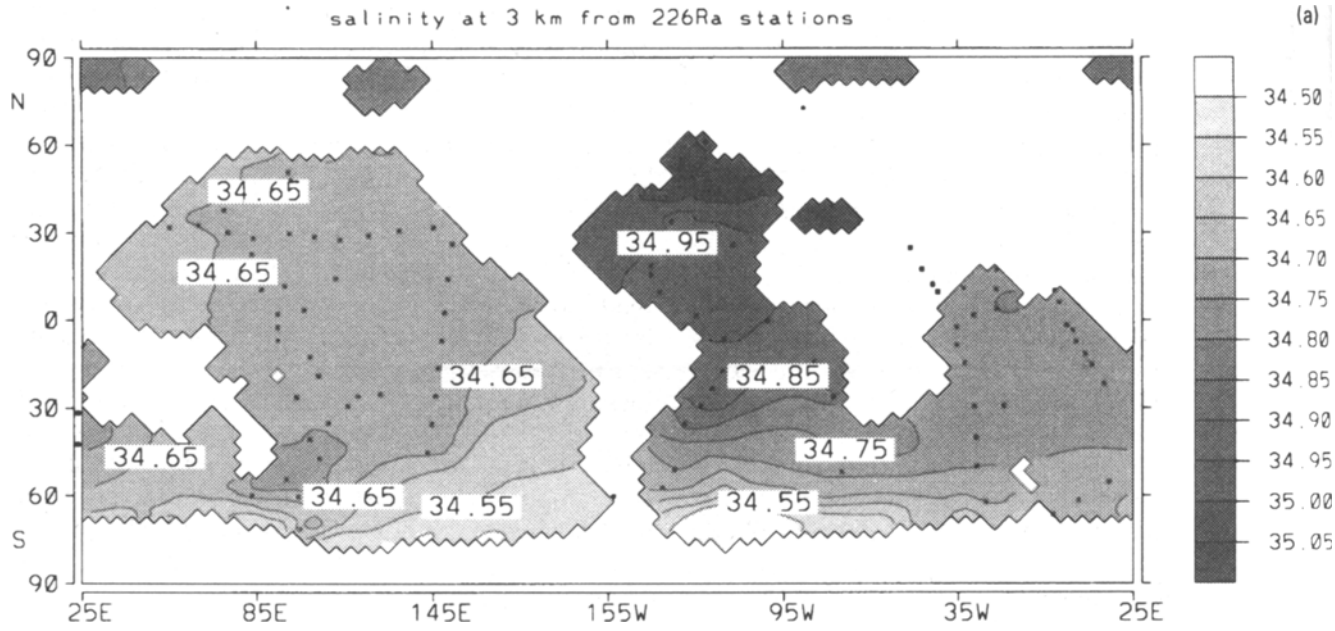

Figure 1(a). Reconstruction of salinity under the assumption that measurements were only available at stations where ^{226}Ra data exist.

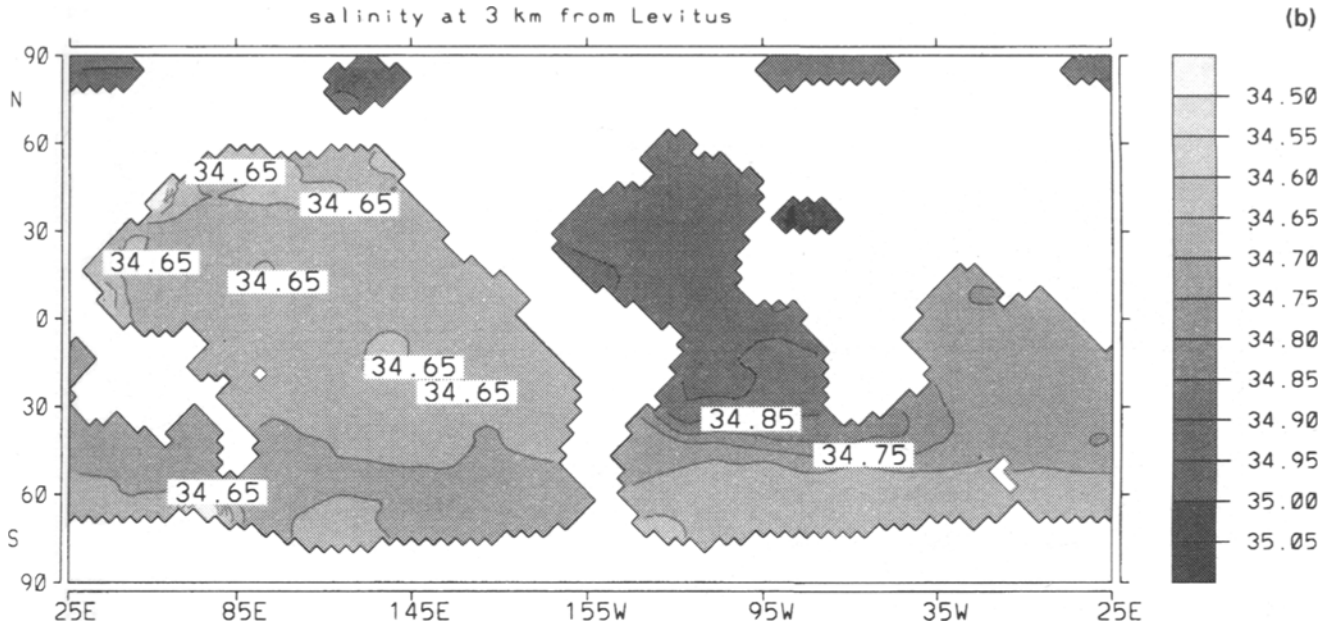

Figure 1(b). Salinity from the Levitus atlas interpolated on the grid of the model.

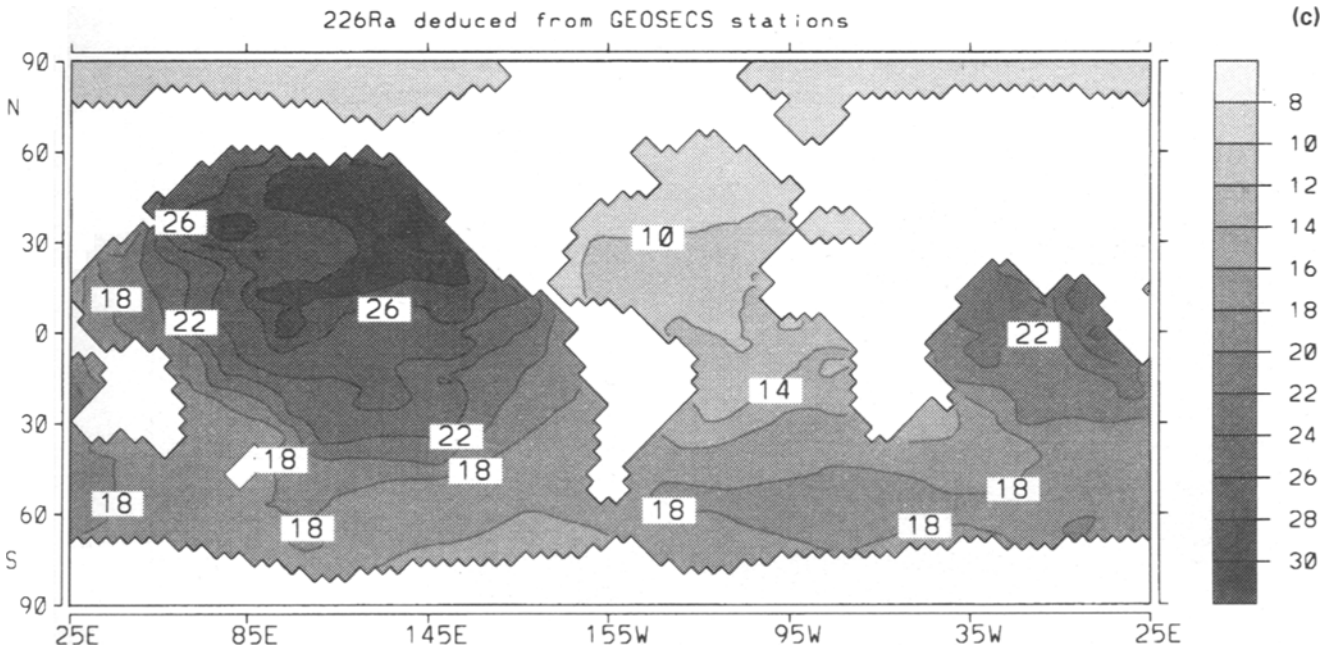

Figure 1(c). Reconstructed distribution of ^{226}Ra at 2 km depth. Units are dpm/100 kg.

more or less based on a concept of isotropic diffusion of the information into space. More realism may be expected from a technique by which the circulation field of a model, once it is accepted to represent essential aspects of the global circulation, is used as an interpolator. The observational information is propagated up- and downstream the models streamline. The space is filled up completely with information by the models diffusivity. Figure 1(a) displays a reconstruction of the salinity field in 1 km depth, based on the hypothetical assumption that salinity measurements were available only at those positions where ^{226}Ra measurements were made. The agreement with the observed salinity distribution is, of course, not perfect; as a result from a GCM it would hardly be taken as acceptable. The dots indicate the positions of data. The global aspects such as the excess salinity of the Northern Atlantic relative to the rest of the deep ocean, however, are captured. In contrast, figure 1(b) displays the distribution of salinity from Levitus (1983) as interpolated onto the grid of our model. Obviously, the streamline interpolation gives a fair reproduction of the known field of salinity. Regional features like the spreading of Mediterranean water in the Atlantic (the centre of the plume is not matched by one of the stations), however, are underrepresented.

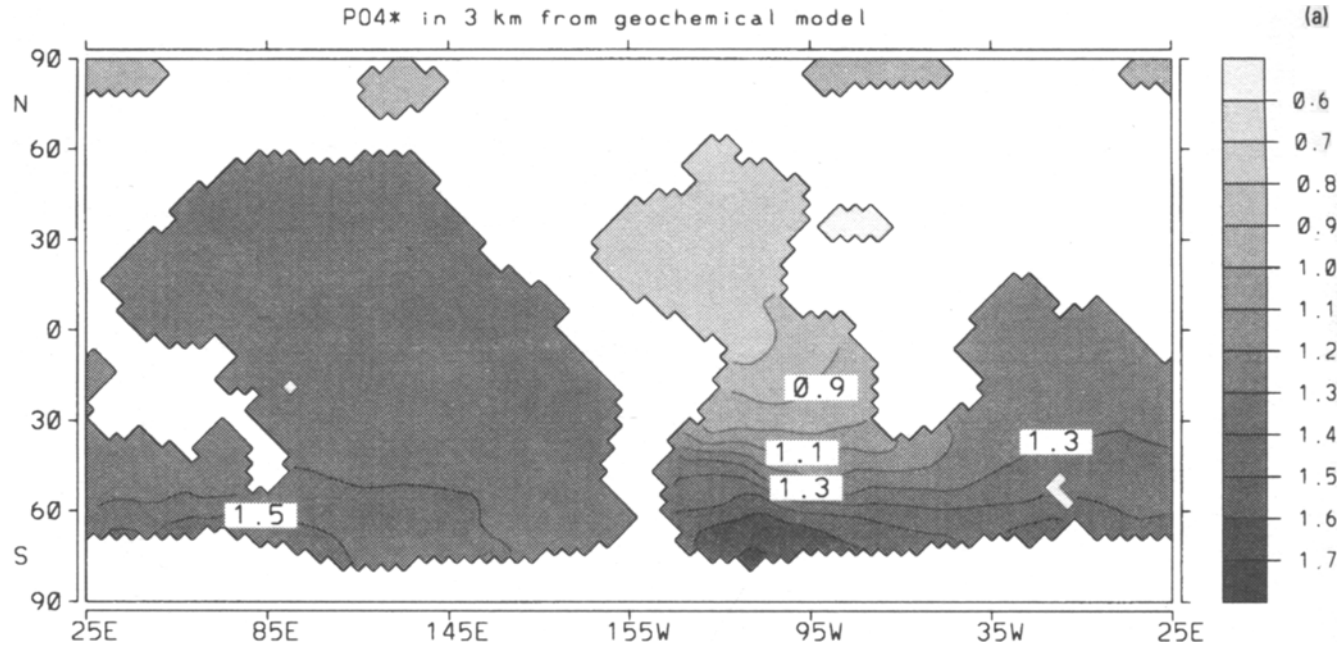

Figure 2(a). Distribution of the models PO_{4^*} at 3 km depth, the center depth of NADW. Note the homogeneous pattern in the Northern Pacific with 1/3 of NADW and 2/3 of Antarctic deep water.

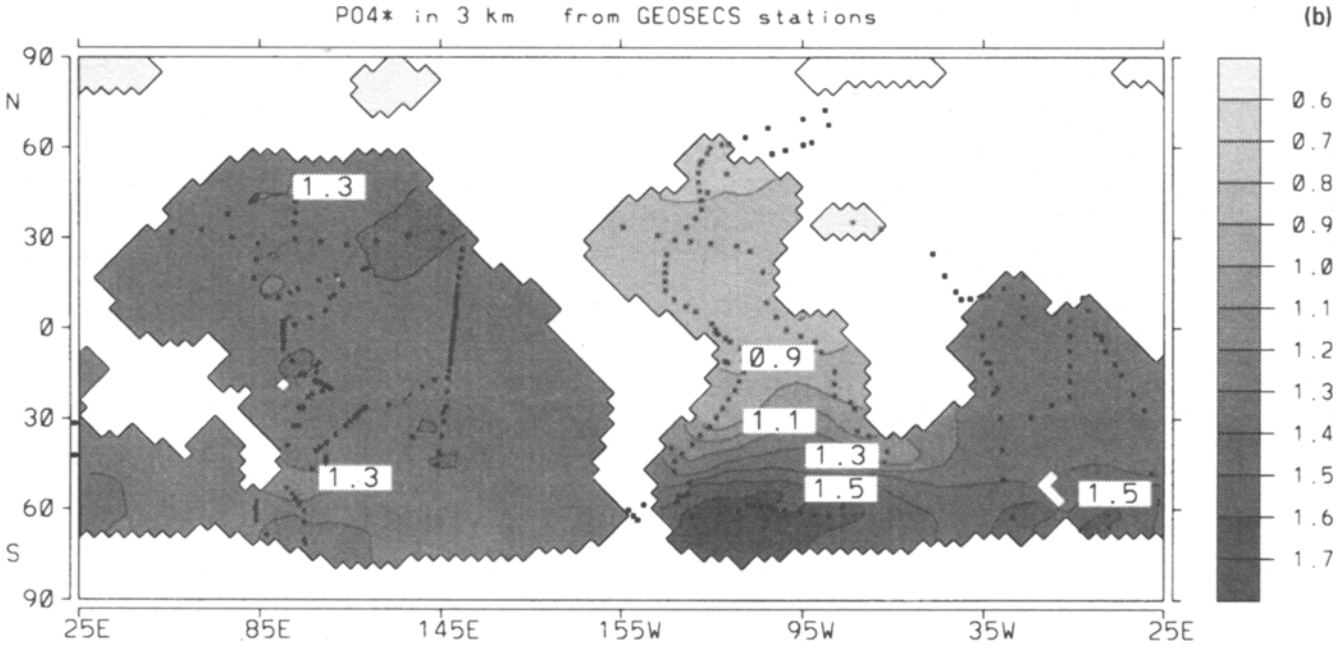

Figure 2(b). Reconstruction of PO_{4^*} from 10399 GEOSECS stations.

It may be expected that for a sparsely measured tracer like ^{226}Ra the representation of the real but unknown field has a similar degree of realism. Figure 1(c) displays the corresponding distribution of ^{226}Ra in 1 km depth.

The realism of the global deep circulation pattern is confirmed by the distribution of

$$PO_{4^*} = PO_4 + O_2/172 - 1.95\mu/l,$$

a combination of phosphate and oxygen that does not change during remineralization of sinking organic debris (Broecker *et al* 1991).

As compared with salinity, PO_{4^*} has the advantage that the magnitudes of the deep sea gradients are more than half the amplitude of the sea surface gradients. It enters the deep ocean in the regions of deep water formation in the Northern Atlantic and around Antarctica, primarily in the Weddell Sea. The distribution is characterized by the mixing between the low values of the northern endmember and the high values of the southern component. Fortunately (from the modeler's point of view), it reacts not very sensitively to the details of the biological production scheme; it can be considered, thus, as a predominantly

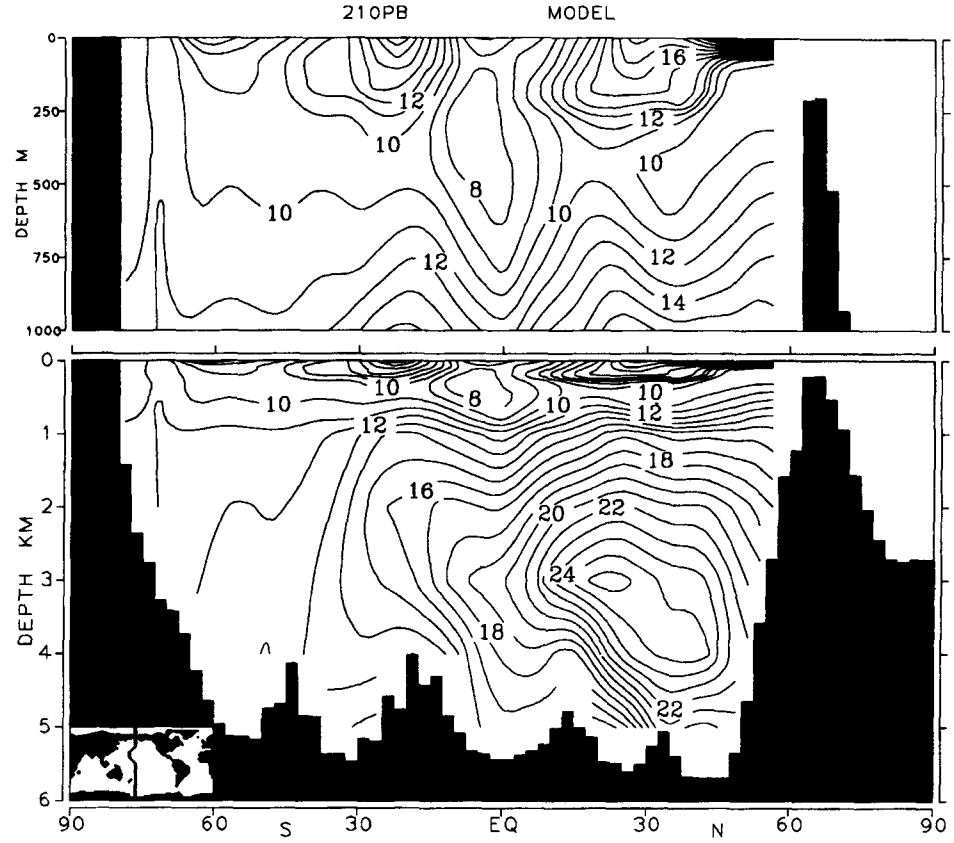

Figure 3. Section of ^{210}Pb in the Western Pacific as given in the ikon. Units are dpm/100 kg.

physical tracer which mirrors the model's deep circulation and mixing properties. Production is simulated by removal of phosphate from the surface with a globally uniform time constant of four months which is locally modified by temperature and mixing conditions. The time constant of four months was chosen to match realistic numbers of phosphate minima in the subtropical gyres (Maier-Reimer 1993). No restoring to observations is performed. Figure 2(a) shows the model's prediction of PO_4^* at a depth horizon of 3 km, which can be directly compared with the corresponding figure from Broecker *et al* (1991), or with the result of the dynamic interpolation of 10399 GEOSECS data with our circulation field. The quantitative simulations of the end member values (0.7 in the Northern Atlantic and 1.7 in the Weddell Sea) is to some extent dependent on the tuning process, but it turned out that this tracer is rather insensitive to the details of biological parameterization. The spreading and mixing into the regions far away from the deep water production represents an independent test of the model's deep circulation.

3. Simulation of ^{210}Pb

For ^{210}Pb the situation is more complex than for ^{226}Ra. Due to the short half-lifetime of 22.3 years, and due to affinity to sinking particles, the interpolation along streamlines is inappropriate. The merit of the model now lies in the determination of the scavenging rates: as the carbon cycle model (Maier-Reimer 1993) from group III predicts realistic distributions of deep oxygen, phosphate, and alkalinity which are determined by the divergence of the fluxes of organic carbon and of calcareous shells, the model can be run in a prognostic mode, tuning the scavenging rates to match the few observed profiles of ^{210}Pb. The model predicts fluxes of organic material, opal, and calcareous shells. In order to minimize the number of free parameters we assume that ^{210}Pb scavenging depends only on the total mass flux of particles and is not affected by the chemistry of these particles. An additional scavenging mechanism is exerted in the deep sea by the contact of dissolved lead with sediment material, as postulated by Spencer *et al* (1981). The tuning of the scavenging rates was obtained in a series of 60-years simulation (3 half-life times), starting from a first guess simulation, where the sum of squares of discrepancies between available data and corresponding model values was minimized. The resulting rms error of individual stations is 1.8 dpm/100kg, i.e. appr. 10% of typical absolute values.

We restrict our discussion of the results on a very few aspects here. Figure 3 shows the simulated distribution of ^{210}Pb along a section in the western Pacific (outlined in the ikon in the left bottom corner). The basic features of the surface maximum (due to eolian

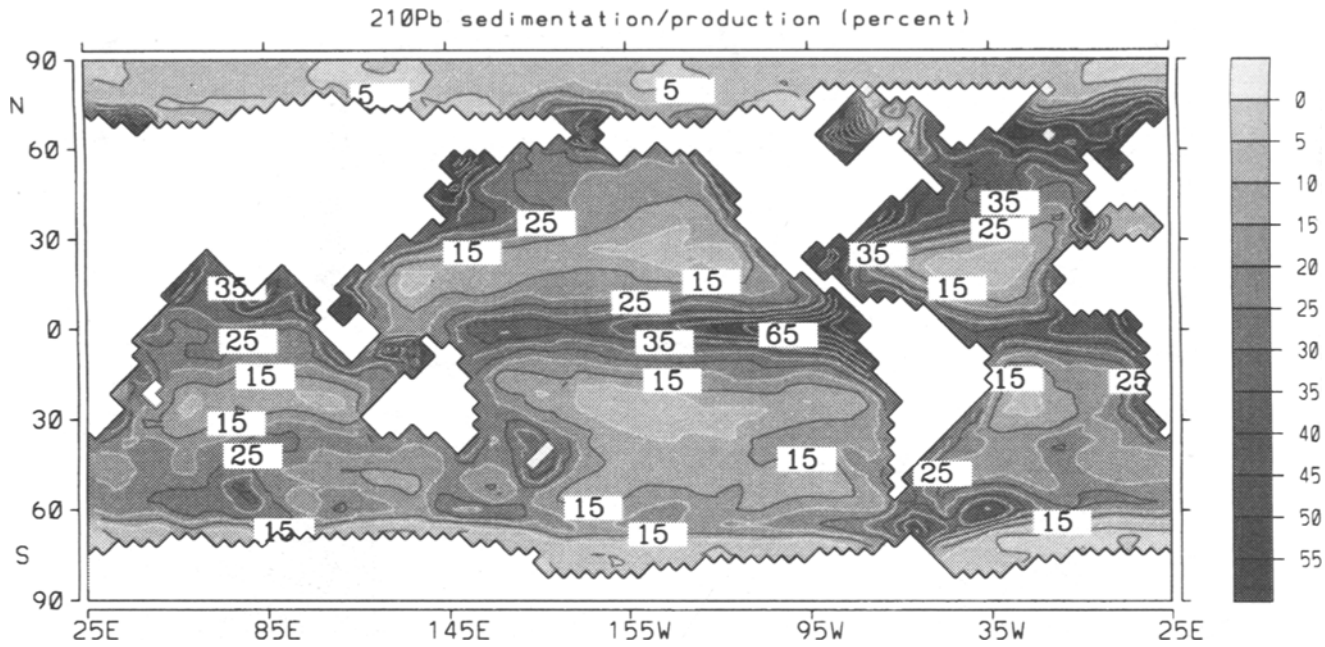

Figure 4. Sedimentation vs. depth-integrated production of ^{210}Pb.

input) and an intermediate maximum at appr. 3 km are reproduced well. The position and strength of the deep maximum – apparently at the same level as the alkalinity maximum – depends delicately on circulation properties, particle flux divergence, and the tuned scavenging rates.

Figure 4 shows the relationship of sedimentation to the depth integrated production. The figure clearly displays regions of high productivity where strong particle fluxes provide a rather high scavenging, and thus, sedimentation rate. In the subtropical gyres the sedimentation rate is rather low, and the production rate for ^{226}Ra is thus rather high. Again due to the low particle flux, the scavenging rate is rather small and most of the loss of ^{210}Pb is due to radioactive decay. Lateral advection (not discussed here) provides a smearing between these two extreme types of local dynamics.

A peculiar feature in figure 4 consists of the low values around Antarctica. This is partly due to the extremely low (except downstream of Australia and Patagonia) eolian input. On the other hand, the Southern Ocean is known to be the most prominent HNLC (high nutrient low chlorophyll) region of the World Ocean, i.e. the biological production is – for whatever reasons – much lower than would be expected from the nutrient supply. Candidates for an explanation of this behaviour are, e. g., unfavourable physical environmental conditions or the lack of iron as a micronutrient due to low dust input. This question is subject to an ongoing vivid scientific debate.

4. Conclusion

As the model provides a ^{210}Pb distribution close to that observed we have some confidence that it is advecting and removing ^{210}Pb in a realistic manner. As the other Pb isotopes are expected to be advected and removed in a similar fashion, this provides the potential to investigate the natural stable Pb isotope distribution in the ocean with two of its three controls understood. This investigation will be the subject of future papers.

References

Abouchami W and Goldstein S L 1995 A lead isotopic study of circum-antartic manganese nodules; *Geochimica et Cosmochimica Acta* **9**

Broecker W S, Blanton S, Smethie W M and Östlund G 1991 Radiocarbon decay and oxygen utilization in the deep Atlantic Ocean; *Glob. Biogeochem. Cycles* **5** 87–117

Christensen J N, Halliday A N, Godfrey L V, Hein J R and Rea D K 1997 Climate and ocean dynamics and the lead isotopic records in Pacific ferromanganese crusts; *Science* **277** 913–918

Cochran J K, McKibbin-Vaughan T, Dornblaser M M, Hirschberg D, Livingston H D and Buesseler K D 1990 ^{210}Pb scavenging in the North Atlantic and North Pacific oceans; *Earth Planet. Sci. Lett.* **97** 332–352

Levitus S 1983 Climatological atlas of the World Ocean; *NOAA Prof. Paper No. 13*

Maier-Reimer E 1993 Geochemical cycles in an ocean general circulation model – Preindustrial tracer distributions; *Glob. Biogeochem. Cycles* **7** 645–677

Maier-Reimer E, Mikolajewicz U and Hasselmann K 1993 Mean circulation of the Hamburg LSG OGCM and its sensitivity to the thermohaline surface forcing; *J. Phys. Oceanogr.* **23** 731–757

O'Nions R K, Frank M, von Blanckenburg F and Ling H-F 1998 Secular variation of Nd and Pb isotopes in ferromanganese crusts from the Atlantic, Indian and Pacific Oceans; *Earth Planet. Sci. Lett.* **155** 15–28

Peng T H, Maier-Reimer E and Broecker W S 1993 Distribution of ^{32}Si in the World Ocean: Model compared to Observation; *Glob. Biogeochem. Cycles* **7** 463–474

Preiss N and Genthon C 1997 Use of a new database of lead 210 for global aerosolmodel validation; *J. Geophys. Res. Atm.* **102** 25347–25357

Sarkisyan A S 1969 Theory and computation of ocean currents; *US Dept. Comm. Springfield, VA*

Spencer D W, Bacon M P and Brewer P G 1981 Models of the distribution of ^{210}Pb in a section across the north equatorial Atlantic Ocean; *J. Mar. Res.* **39** 119–138

Toggweiler J R, Dixon K and Bryan K 1989 Simulations of radiocarbon in a coarse-resolution World Ocean model 1: Steady state prebomb distributions; *J. Geophys. Res.* **94** 8217–8242

von Blanckenburg F, O'Nions R K and Hein J R 1996 Distribution and sources of preanthropogenic lead isotopes in deep ocean water from Fe-Mn crusts; *Geochim. Cosmochim. Acta* **60** 4957–4964